Dispersive and steady-state recombination in organic disordered semiconductors

Andreas Hofacker[1,*] and Dieter Neher[2,†]

[1]*Dresden Integrated Center for Applied Physics and Photonic Materials (IAPP) and Institute for Applied Physics, Technische Universität Dresden, 01187 Dresden, Germany*

[2]*Department of Physics and Astronomy, Universität Potsdam, 14476 Potsdam, Germany*

(Received 25 October 2017; revised manuscript received 27 November 2017; published 27 December 2017)

Charge carrier recombination in organic disordered semiconductors is strongly influenced by the thermalization of charge carriers in the density of states (DOS). Measurements of recombination dynamics, conducted under transient or steady-state conditions, can easily be misinterpreted when a detailed understanding of the interplay of thermalization and recombination is missing. To enable adequate measurement analysis, we solve the multiple-trapping problem for recombining charge carriers and analyze it in the transient and steady excitation paradigm for different DOS distributions. We show that recombination rates measured after pulsed excitation are inherently time dependent since recombination gradually slows down as carriers relax in the DOS. When measuring the recombination order after pulsed excitation, this leads to an apparent high-order recombination at short times. As times goes on, the recombination order approaches an asymptotic value. For the Gaussian and the exponential DOS distributions, this asymptotic value equals the recombination order of the equilibrated system under steady excitation. For a more general DOS distribution, the recombination order can also depend on the carrier density, under both transient and steady-state conditions. We conclude that transient experiments can provide rich information about recombination in and out of equilibrium and the underlying DOS occupation provided that consistent modeling of the system is performed.

DOI: 10.1103/PhysRevB.96.245204

I. INTRODUCTION

Solid samples of organic semiconductors (OSCs) exhibit energetic and positional disorder due to their intramolecular and intermolecular degrees of freedom. The electronic structure of solid OSCs is, therefore, best described by an inhomogeneously broadened density of localized states, where states in the tail of the distribution act as temporary traps. The motion of charge carriers in such systems is typically treated by considering hopping between localized sites, with no contribution from coherent transport.

Numerous experimental and theoretical papers dealt with hopping transport in solid OSCs, covering the time scale from femtoseconds to the steady state [1–4]. A common observation (prediction) was that if charges were introduced into the solid OSC through photogeneration or injection, they were very mobile at the beginning, but slowed down progressively while occupying states deeper and deeper in the density of states (DOS) distribution. This so-called dispersive transport carries important information on the shape of the DOS [5–7]. Similarly, the characteristic dependence of steady-state mobility on electric field, temperature, and carrier density was often employed to characterize the distribution of transport sites in space and energy [8,9].

Surprisingly, fewer publications dealt with the effect of disorder on the nongeminate recombination of charges in photoactive organic photovoltaic (OPV) layers, despite its importance in limiting the photovoltaic performance. Several studies considered how disorder affects the steady-state properties, in particular the ideality factor and the apparent order of recombination, but with a focus on a particular shape of the DOS (Gaussian or exponential) or a particular recombination mechanism (e.g., free with trapped charge) [10–13].

Even less is known about the role of disorder in the time dependence of nongeminate recombination. On the experimental side, the temporal evolution of photoexcited species in neat conjugated polymers was attributed to bimolecular recombination in a Gaussian distribution of localized states [14–16]. Similarly, Gaussian or exponential state distributions were employed to understand the time dependence of nongeminate recombination of photogenerated charge in some donor-acceptor bulk heterojunction systems [17–20].

On the theoretical side, the effect of disorder on nongeminate recombination has been treated in and starting from a steady state [21–24]. These treatments, however, did not capture the rich nonequilibrium nature of the dynamics following short-pulse excitation. When describing the time development after pulsed excitation, a suitable model had to account for recombination and relaxation simultaneously. The work of Orenstein and Kastner [25] can be viewed as pioneering in this respect since it treated energetic thermalization and higher-order recombination together for the first time. Their analysis was, however, limited to an exponential DOS and can furthermore not be applied in the case of low recombination rates [25,26]. A very elaborate paper was published by Tachiya and Seki [27], who also combined thermalization and recombination in their calculations, but again limited themselves to an exponential DOS. They compared their analytical results to kinetic Monte Carlo simulations [17] of the same model system. Recently, the influence of the spatial distribution of the carrier density on the transient and steady-state recombination dynamics in heterojunction solar cells was studied using numerical and analytical methods [12,28]. A general description of the influence of the density of localized states on the time development of recombination and thermalization after pulsed excitation is, however, still missing.

*andreas.hofacker@tu-dresden.de
†neher@uni-potsdam.de

Here we present a comprehensive treatment of the effect of the density of localized states on the time dependence of nongeminate recombination and on the relevant steady-state parameters. In contrast to earlier studies, this work treats all relevant regimes, from the early time scale of thermalization to steady state, for different combinations of DOS and considering both free-to-free and free-to-trapped recombination. We show that dispersive recombination is inherent to disordered semiconductors and that the time it takes for the system to attain the asymptotic long-time recombination limit bears information about the shape and energetic width of the state distribution. We also show how characteristic steady-state parameters, such as the ideality factor or the recombination order, depend on the choice of the DOS and of the recombination pathway, and that the measurement of only one of these parameters may not provide sufficient information.

II. TIME-DEPENDENT RECOMBINATION RATES

The time development of the carrier density which is subject to recombination and thermalization can be described by the multiple trapping (MT) formalism, which is an equivalent formulation of the transport energy (TE) model. The TE model is based on the observation that a carrier which is localized in a low-energy state will, before it can move further, perform a hop to a state with energy close to a certain level ε_t, the so-called *transport energy*.

The value of ε_t is independent of the starting energy of the hop and specific to the DOS of the material. There are various calculations of ε_t available in literature [29–32]. We will, for simplicity, assume $\varepsilon_t = 0$ when defining the DOS distributions.

Since the thermal activation to ε_t is the limiting step for transport, one distinguishes between the *free* carrier density n of carriers close to ε_t and the *total* carrier density N. The probability of a state with a given energy ε to be occupied is defined as the occupation function $f(\varepsilon)$. The majority of carriers will reside in low-energy states with $\varepsilon < \varepsilon_t$ and we call them *trapped*.

If a carrier is activated to ε_t, it can either move to a low-energy state again or recombine. For calculating recombination rates, let us consider two possible pathways: recombination of free with free carriers and recombination of free with all carriers of the opposite type. We will call the latter the *free-trapped* recombination. In most situations, the free-trapped case seems more realistic, since if, e.g., an electron becomes mobile, it has the possibility to move towards a hole, whether the hole is mobile or not. One can, however, imagine cases where only the fraction of mobile carriers of both types can take part in recombination, e.g., in a phase-separated geometry with electrons and holes trapped in different phases. We want to investigate both pathways, acknowledging that it will depend on the specific system, which picture is more applicable.

To study the recombination dynamics of the system, we investigate the recombination rate dN/dt as a function of N. Let us assume that the total electron density N is equal to the total hole density P. This assumption is not necessary but will simplify the notation in the following. In general, recombination will then be described by a rate equation of the form

$$\frac{dN}{dt} = -k_r N^{\delta}, \tag{1}$$

where k_r is the recombination rate coefficient and we call δ the *recombination order*. As we will show below, both k_r and δ are, in general, inherently time dependent.

A. Two ways to solve the transport energy problem

In this section we will describe two approaches to solve the TE problem: solving the full MT equations and using the effective energy [26] ε^*.

The full MT equations, which we choose to write for electrons, for concreteness, read

$$\frac{dn}{dt} = \int_{-\infty}^{0} \nu_{\text{detrap}}(\varepsilon) f(\varepsilon) g(\varepsilon)\, d\varepsilon - b_t \int_{-\infty}^{0} [1 - f(\varepsilon)] g(\varepsilon)\, d\varepsilon - b_r n P_{\text{eff}}, \tag{2}$$

$$\frac{df(\varepsilon)}{dt} = b_t [1 - f(\varepsilon)] n(t) - \nu_{\text{detrap}}(\varepsilon) f(\varepsilon) - b_r p f(\varepsilon), \tag{3}$$

with the detrapping rate $\nu_{\text{detrap}}(\varepsilon) = \nu_0 \exp[\varepsilon/kT]$, the attempt-to-escape frequency ν_0, the trapping rate constant b_t, the recombination rate constant b_r, the free electron and hole densities n and p, and the hole density that is effective for recombination with free electrons P_{eff}, which could be the free or the total hole density. Note that in Eq. (3) we neglect the recombination of trapped electrons with trapped holes since we consider trapped charges as immobile.

The same equations have to be solved for holes, simultaneously.

Equations (2) and (3) are defined for a general DOS $g(\varepsilon)$. In this paper we will focus on two exemplary DOS distributions—the Gaussian and the exponential DOS—since they are widely accepted for the description of disordered semiconductors. The Gaussian DOS is defined as

$$g(\varepsilon) = \frac{N_t}{\sigma\sqrt{2\pi}} \exp\left(-\frac{\varepsilon^2}{2\sigma^2}\right), \tag{4}$$

while the exponential DOS is given by

$$g(\varepsilon) = \frac{N_t}{\varepsilon_0} \exp\left(\frac{\varepsilon}{\varepsilon_0}\right). \tag{5}$$

In both cases, N_t is the density of states, integrated over ε. σ and ε_0 are the standard deviations of the respective distributions.

The MT problem can be transparently solved by introducing an effective energy ε^* as shown in Ref. [26]. Using the ε^* picture it is possible to derive analytical expressions for the long-time recombination rate, including the long-time recombination order. We are also able to clarify the qualitative behavior of the carrier distributions depending on time, carrier density, and the DOS.

The effective energy ε^* denotes the cutoff energy of the occupation function that is assumed to be step-like in energy. Consequently, since the DOS decreases rapidly into the energy gap, most charge carriers will reside in states with energy close to ε^*.

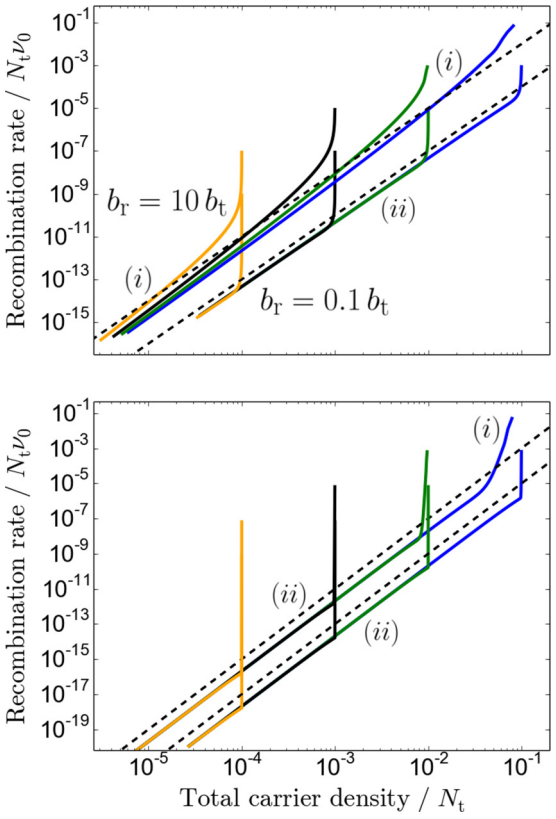

FIG. 1. Recombination rate $R = |dN/dt|$ as a function of carrier density after pulsed excitation for different initial densities in an exponential DOS. Top: free-trapped; bottom: free-free recombination. $\varepsilon_0 = 2\,kT$ for all curves. The solid lines are calculated from Eqs. (2) and (3), the dashed lines from Eqs. (19) and (22), respectively. In all four panels of Figs. 1 and 2, $b_r/b_t = 10$ for the upper family of curves and 0.1 for the lower.

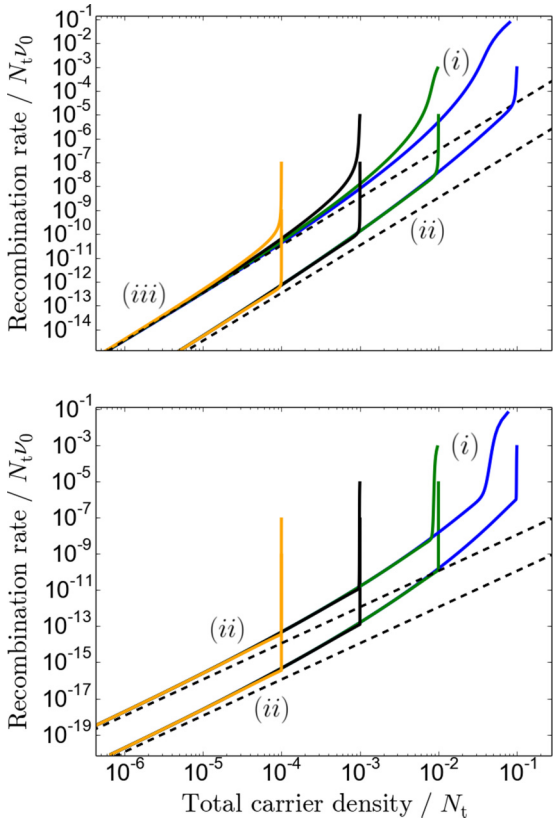

FIG. 2. Recombination rate $R = |dN/dt|$ as a function of carrier density after pulsed excitation for different initial densities, in a Gaussian DOS. Top: free-trapped; bottom: free-free recombination. $\sigma = 4\,kT$ for all curves. The solid lines are calculated from Eqs. (2) and (3), the dashed lines from Eqs. (13) and (14), respectively.

In the free-trapped recombination case, the dynamics of ε^* and the total carrier density N can be described by the following two rate equations [26]:

$$\frac{dN}{dt} = -b_r N^2(t)\gamma(\varepsilon^*), \tag{6}$$

$$\frac{d\varepsilon^*}{dt} = -\frac{\gamma(\varepsilon^*)}{g(\varepsilon^*)}G(\varepsilon^*)N(t)\left[b_r - b_t + b_t\frac{G(\varepsilon^*)}{N(t)}\right], \tag{7}$$

with

$$G(\varepsilon^*) = \int_{-\infty}^{\varepsilon^*} g(\varepsilon)d\varepsilon, \tag{8}$$

$$\gamma(\varepsilon^*) = \exp[\varepsilon^*/kT]\frac{g(0)}{g(\varepsilon^*)}. \tag{9}$$

Here $G(\varepsilon^*)$ is the density of states below ε^* and $\gamma(\varepsilon^*)$ is the ratio of the free carrier density n at the transport level to the total carrier density N, assuming that most carriers are situated in a narrow energy interval around ε^*. For more details on the ε^* approach, refer to Ref. [26].

In the case of free-free recombination, assuming the same $g(\varepsilon)$ for electrons and holes Eqs. (6) and (7) transform into

$$\frac{dN}{dt} = -b_r N^2(t)\gamma^2(\varepsilon^*), \tag{10}$$

$$\frac{d\varepsilon^*}{dt} = -\frac{\gamma(\varepsilon^*)}{g(\varepsilon^*)}G(\varepsilon^*)N(t)\left[b_r\gamma(\varepsilon^*) - b_t + b_t\frac{G(\varepsilon^*)}{N(t)}\right]. \tag{11}$$

B. Dispersive recombination rates

Let us put our system in the following situation: It is subject to a pulsed excitation (e.g., photoexcitation by a short laser pulse) and then left to thermalize. After a certain delay time the total charge carrier density is measured. From these $N(t)$ data we can derive $[dN/dt](t)$ and thus also $[dN/dt](N)$ data. With this, we can visualize Eq. (1) by plotting dN/dt versus N.

Figures 1 and 2 compile such plots of the recombination rate versus the carrier density for the two DOS distributions Eqs. (4) and (5) and both free-trapped and free-free recombination. Solid lines are calculated from the full MT equations, Eqs. (2) and (3), the dashed lines are analytical asymptotes calculated with the ε^* approach as outlined in Sec. III.

Each calculation is done for different initial densities $N(0)$ and for the cases $b_r/b_t > 1$ and $b_r/b_t < 1$. This ratio is of great importance for the nonequilibrium behavior of the recombination rate, as we will show below. Since the plots in

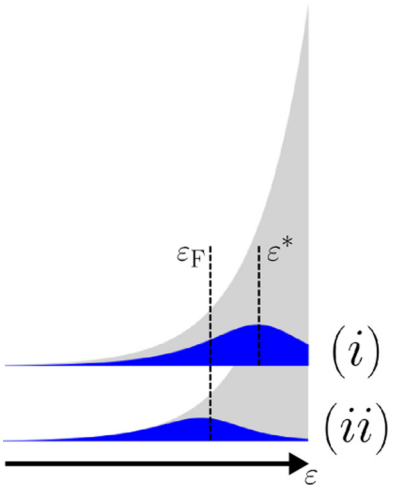

FIG. 3. Different configurations of a carrier packet (DOOS, blue) in an exponential DOS (gray). The peak of the DOOS is approximated by ε^*. Top: Nonthermalized carriers with $\varepsilon^* >$ "ε_F" [regime (i)]. Bottom: Thermalized carriers with $\varepsilon^* = \varepsilon_F$ [regime (ii)].

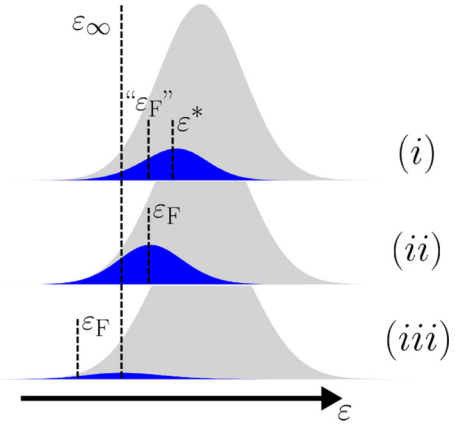

FIG. 4. Different configurations of a carrier packet (DOOS, blue) in a Gaussian DOS (gray). The peak of the DOOS is approximated by ε^*. Top: Nonthermalized carriers with $\varepsilon^* > \varepsilon_\infty$ and $\varepsilon^* > \varepsilon_F$ [regime (i)]. Middle: Thermalized carriers with $\varepsilon^* = \varepsilon_F$ [regime (ii)]. Bottom: Carriers with $\varepsilon^* = \varepsilon_\infty$, which could be thermalized or nonthermalized [regime (iii)].

Figs. 1 and 2 are logarithmic, the slope of the curves equals δ as defined by Eq. (1). It has to be kept in mind that in this time-dependent paradigm high carrier densities, where only little recombination has yet taken place, correspond to short delay times. We thus read Figs. 1 and 2 always from right to left, i.e., from high to low carrier densities.

For analyzing the transients we have to introduce three more terms: the *quasi-Fermi-level*, the *hypothetical* quasi-Fermi-level, and the *equilibration energy*. When a quasi-Fermi-level exists, thermal quasi-equilibrium [33] is established within the density of states of the respective excited carrier type. By hypothetical quasi-Fermi-level, we mean the value of ε_F that would be the parameter of a Fermi-Dirac distribution $f_{FD}(\varepsilon;\varepsilon_F)$ that satisfies the condition

$$N = \int_{-\infty}^{\infty} f_{FD}(\varepsilon;\varepsilon_F)\, g(\varepsilon)\, d\varepsilon. \tag{12}$$

This value is also defined if the system is not in thermal equilibrium and we can use it to describe the state our system is in. We will thus use the general definition of ε_F via Eq. (12) in all cases and, if relevant, state if equilibrium is actually established. Note that the exponential DOS as defined by Eq. (5) is not meaningful for energies far above ε_t and only describes the DOS tail. This is, however, not a problem for Eq. (12) since $f_{FD} \cdot g$ tends to zero exponentially above $\varepsilon = 0$ for $\varepsilon_0 > kT$.

The equilibration energy ε_∞ exists in DOS distribution that are at least as steep as the Gaussian [1,34], due to the competition of the occupation function and the DOS. Since the occupation function typically decays not faster than exponentially towards high energies, the product with a DOS that depends on energy more steeply yields a density of occupied states with a peak at ε_∞, provided that ε_∞ lies in the decaying region of the occupation function. For the Gaussian DOS, $\varepsilon_\infty = -\sigma^2/kT$. Consequently, a thermalizing carrier packet will not relax to energies below ε_∞ but rather be stopped at this energy, only able to change its energetic width and, if recombination occurs, carrier density. If quasi-equilibrium is then attained, the packet assumes a Gaussian distribution with a width σ_{occ} equal to the width of the DOS σ.

With the help of ε^*, ε_F and, in the case of a Gaussian DOS, ε_∞, different regimes can be identified (see Figs. 3 and 4). We start with the exponential DOS, Fig. 1.

In the early stage, right after pulsed excitation, the system is far out of equilibrium [regime (i)]. Here ε^* is larger than ε_F as shown in Fig. 3. The recombination rate is high and thermalization has only started. Due to fast initial thermalization to low-energy states, the recombination rate drops rapidly, which, in combination with only a small change in carrier density due to recombination, dupes a high recombination order. In this early time region, the recombination rate does not only depend on N, but also on time, meaning that the recombination rate can be different at the same N, if the initial density $N(0)$ is different. This is the regime of dispersive recombination of nonthermalized charge.

If, as time progresses, the individual traces which only have different $N(0)$ merge, the recombination rate only depends on N and not on time from there on. This is when quasi-equilibrium is attained, meaning that $\varepsilon^* = \varepsilon_F$. This is regime (ii). At this point, the recombination rate is an explicit function of the total carrier density only. Importantly, for the exponential DOS the slope of the merged $R(N)$ curves (the recombination order) is independent of carrier density.

However, there is also a case, where the $R(N)$ curves approach a constant recombination order, but do not merge into one curve. That is the case of $b_r > b_t$ for free-trapped recombination in the exponential DOS (Fig. 1, top). Here, quasi-equilibrium is never established after pulsed excitation, as we will discuss in Sec. III D, and regime (i) of Fig. 3 persists for all times. Interestingly, the asymptotic recombination order is equal to that of the equilibrated case, which is a special property of the exponential DOS (cf. Sec. III D).

The case of the Gaussian DOS is more complicated because of the existence of ε_∞. Here it is possible that thermal quasi-equilibrium is established before ε_F reaches ε_∞. Then $\varepsilon^* = \varepsilon_F > \varepsilon_\infty$. This is regime (ii) in Fig. 4, similar to the

exponential DOS. The recombination rate will be a function of carrier density only, but in contrast to an exponential DOS, the recombination order will also dependent on N (which is an explicit function of $\varepsilon^* = \varepsilon_F$).

We finally observe a second transition from regime (ii) to (iii). Here ε_F sinks due to recombination, but ε^* gets pinned at ε_∞ [regime (iii)]. This transition manifests in the $R(N)$ plots as the approach of a constant slope of 2 by the already merged curves over several orders of magnitude of the carrier density. The fact that the latter transition of the merged curves exists for the Gaussian DOS, but not for the exponential DOS, is due to the absence of a special energy like ε_∞ in the exponential DOS, and thus also the absence of regime (iii).

It, however, is also possible that ε_F sinks below ε_∞ before thermal equilibrium can be established. Later, ε^* reaches ε_∞ and gets pinned there. Thus, an additional transition from regime (i) directly to regime (iii) is possible, which happens for fast recombination like in Fig. 2, top, for $b_r = 10b_t$. This behavior is reflected in the fact that the asymptotic recombination order is reached before the curves with different $N(0)$ merge.

Thermal equilibrium then might or might not be established at some later time, depending on b_r/b_t. Interestingly, the asymptotic recombination order is the same in both cases since the long-time energetics of the Gaussian DOS are governed by ε_∞ alone.

For free-free recombination, the recombination rates are generally lower than for free-trapped recombination (if all other parameters are unchanged) since less carriers can take part in recombination events. Therefore quasi-equilibrium is always attained. This can also be rationalized from inspecting Eq. (10), where recombination slows down quadratically with $\gamma(\varepsilon^*)$, while in Eq. (11), the change rate of ε^* still contains terms with are linear in $\gamma(\varepsilon^*)$. In Sec. VI we show rigorously that this is especially true for continuous carrier generation.

In summary, the transitions between the presented regimes depend largely on the nature of the DOS, whether free-free or free-trapped recombination is present, and whether b_r is smaller or larger than b_t.

We will elaborate on the origins of the transient behavior and calculate the asymptotic long-time slopes, i.e., values of δ, in Sec. III. In Sec. IV, we will derive estimates of the time scale of approaching the asymptotic δ and the fraction of carriers that have recombined until then. Finally, in Sec. VI we will calculate the recombination orders and ideality factors of solar cells made from such materials and compare them to the values of δ obtained from the transient technique described above.

III. LONG-TIME LIMIT OF TRANSIENT RECOMBINATION

Let us calculate the recombination rates in the long-time limit for the case that electrons and holes both move in the same Gaussian or exponential DOS in Secs. III A and III B. In Sec. III C we will treat the general case of two different DOS distributions and give the result for a Gaussian DOS for electrons and an exponential DOS for holes.

A. Gaussian DOS

Let us start with the Gaussian DOS distribution since it is more easily treated at long times. In the long-time limit for the Gaussian DOS, carriers will be situated at the equilibration energy [1,34] $\varepsilon_\infty = -\sigma^2/kT$.

This is only true if the carrier density is low enough for the quasi-Fermi-level to be deeper than ε_∞. However, after a pulsed excitation, there will always occur a point in time when enough carriers have recombined to ensure that $\varepsilon_F < \varepsilon_\infty$. Then we can replace ε^* by ε_∞ in Eqs. (6) and (10), yielding

$$\frac{dN}{dt} = -b_r N^2(t) \exp\left[-\frac{1}{2}\left(\frac{\sigma}{kT}\right)^2\right] \tag{13}$$

for the free-trapped recombination and

$$\frac{dN}{dt} = -b_r N^2(t) \exp\left[-\left(\frac{\sigma}{kT}\right)^2\right] \tag{14}$$

for the free-free recombination pathway.

The fact that $\gamma(\varepsilon^*)$ does not depend on N or time in the long-time limit means that then the free carrier density is proportional to N, rendering the recombination kinetics bimolecular, i.e., $dN/dt \propto N^2$, for both pathways.

Equations (13) and (14) are plotted as the dashed lines in Fig. 2, top and bottom, respectively. The asymptotic behavior of the MT results is accurately reproduced.

B. Exponential DOS

Here we will first treat the case where the system is in quasi-equilibrium. See Sec. III D for a treatment of the opposite case, which occurs when recombination is so fast to prevent equilibration. If the system is equilibrated, the occupation is described by a Fermi-Dirac distribution. The product of this distribution with the DOS yields the density of occupied states which has a peak at ε_F. Thus, at long times after sample excitation, carriers in the exponential DOS will mostly be located in the vicinity of the quasi-Fermi-level ε_F. Thus, we have to replace ε^* by ε_F in Eqs. (6) and (10) to obtain the recombination rates in the long-time limit.

Let us first consider free-trapped recombination. From Eq. (6) we obtain

$$\frac{dN}{dt} = -b_r N^2 \exp\left[\frac{\varepsilon_F}{kT} - \frac{\varepsilon_F}{\varepsilon_0}\right]. \tag{15}$$

We notice that the total carrier density N can be expressed in terms of ε_F, approximating the Fermi-Dirac distribution by a step-distribution with the edge at ε_F:

$$N \approx \int_{-\infty}^{\varepsilon_F} g(\varepsilon) d\varepsilon \tag{16}$$

$$= N_t \exp\left[\frac{\varepsilon_F}{\varepsilon_0}\right]. \tag{17}$$

Thus, Eq. (15) can be rewritten

$$\frac{dN}{dt} = -b_r N^2 \left(\frac{N}{N_t}\right)^{\varepsilon_0/kT} \left(\frac{N}{N_t}\right)^{-1}, \tag{18}$$

$$= -b_r N_t^{1-\varepsilon_0/kT} N^{1+\varepsilon_0/kT}. \tag{19}$$

Again, a power-law dependence of the recombination rate on the total carrier density N is predicted, with the order of recombination equal to $1 + \varepsilon_0/kT$ in this case.

An analogous calculation for free-free recombination yields

$$\frac{dN}{dt} = -b_r N^2 \exp\left[2\frac{\varepsilon_F}{kT} - 2\frac{\varepsilon_F}{\varepsilon_0}\right], \tag{20}$$

$$= -b_r N^2 \left(\frac{N}{N_t}\right)^{2\varepsilon_0/kT} \left(\frac{N}{N_t}\right)^{-2}, \tag{21}$$

$$= -b_r N_t^{2-2\varepsilon_0/kT} N^{2\varepsilon_0/kT}. \tag{22}$$

The recombination order thus equals $2\varepsilon_0/kT$ in the case of free-free recombination in an exponential DOS.

Equations (19) and (22) are plotted as the dashed lines in Fig. 1, top and bottom, respectivley. Again, the asymptotic behavior of the MT results is accurately reproduced. However, there is a small offset between the dashed and solid lines, which is caused by the assumption of a sharp edge of the occupation function $f(\varepsilon)$ at $\varepsilon^* = \varepsilon_F$. This assumption leads to a small (compared to ε_0) overestimation of ε_F and disrupts thermalization at an energy a little above the exact ε_F. Consequently, the recombination rate is also overestimated. The overestimation, however, decreases with increasing ε_0/kT.

C. Different DOS for electrons and holes

In case the two DOS distributions are different for electrons and holes, only the free-free carrier recombination pathway has to be reanalyzed. In the free-trapped case, the calculations of Secs. III A and III B remain valid when choosing the DOS corresponding to the free carrier type. The DOS of the trapped carrier type is irrelevant since they all function as recombination partners, independent of their energy.

In the free-free case, Eq. (10) is rewritten as

$$\frac{dN}{dt} = -b_r N^2(t) \gamma_e(\varepsilon_e^*) \gamma_h(\varepsilon_h^*), \tag{23}$$

with the subscripts e and h labeling electrons and holes, respectively. Choosing, for example, a Gaussian DOS for electrons and an exponential DOS for holes, we obtain

$$\gamma_e(\varepsilon_{\infty,e}) = \exp\left[-\frac{1}{2}\left(\frac{\sigma_e}{kT}\right)^2\right], \tag{24}$$

$$\gamma_h(\varepsilon_{F,h}) = \left(\frac{N}{N_{t,h}}\right)^{\varepsilon_{0,h}/kT} \left(\frac{N}{N_{t,h}}\right)^{-1}, \tag{25}$$

and thus

$$\frac{dN}{dt} = -b_r N_{t,h}^{1-\varepsilon_{0,h}/kT} \exp\left[-\frac{1}{2}\left(\frac{\sigma_e}{kT}\right)^2\right] N^{1+\varepsilon_{0,h}/kT}. \tag{26}$$

The recombination order is governed by the exponential DOS contribution and equals the free-trapped order of the exponential DOS, $1 + \varepsilon_{0,h}/kT$.

D. Long-time limit for fast recombination in the exponential DOS

When the trapping rate constant b_t is very small compared to the recombination rate constant b_r, it can occur, as already shown by Orenstein and Kastner [25], that the (hypothetical) quasi-Fermi-level sinks faster, or equally fast, due to recombination than ε^* (ε_d in Ref. [25]) due to trapping in deep states. In that case, quasi-equilibrium is never established in the transient experiment.

However, we can already see that this does not affect the long-time recombination order for the Gaussian DOS since the free carrier density n is still proportional to the total carrier density N as soon as ε^* crosses ε_∞. Thus, we only have to redo our calculations in the cases where the exponential DOS is governing. We will see that, although the relaxation energetics are different, the recombination order is unchanged compared to the case $b_t \geqslant b_r$.

If $b_t \ll b_r$, ε^* will be much higher in energy than ε_F. Thus the density of states below ε^*, $G(\varepsilon^*)$, is much bigger than the total carrier density N. Using $b_t \ll b_r$ and $G(\varepsilon^*) \gg N$ in Eq. (7) yields the approximation

$$\frac{d\varepsilon^*}{dt} = -\frac{\gamma(\varepsilon^*)}{g(\varepsilon^*)} G^2(\varepsilon^*) b_t, \tag{27}$$

which for the exponential DOS defined by Eq. (5) reads

$$\frac{d\varepsilon^*}{dt} = -\varepsilon_0 b_t N_t \exp\left[\frac{\varepsilon^*}{kT}\right]. \tag{28}$$

The solution of this differential equation is

$$\varepsilon^*(t) = -kT \ln(\nu t), \tag{29}$$

with $\nu = b_t N_t \varepsilon_0/kT$. Inserting this result into Eq. (6), one obtains

$$\frac{dN}{dt} = -b_r (\nu t)^{\alpha-1} N^2(t), \tag{30}$$

with $\alpha = kT/\varepsilon_0$, which is solved by

$$\frac{N(t)}{N(0)} = \frac{1}{(t/\tau)^\alpha + 1}, \tag{31}$$

where

$$\tau = \left(\frac{\alpha\, \nu^{1-\alpha}}{b_r\, N(0)}\right)^{1/\alpha}. \tag{32}$$

We see that since the recombination rate now is explicitly time dependent, we cannot directly deduce a recombination order from Eq. (30). However, for large t, Eq. (31) tells us that $N(t) \propto t^{-\alpha}$. If we substitute $t \propto N^{-1/\alpha}$ into Eq. (30), we obtain for the long-time limit

$$\frac{dN}{dt} \propto N^{1+1/\alpha}, \tag{33}$$

which is exactly the same apparent recombination order $(1 + \varepsilon_0/kT)$ as for the quasi-equilibrated case given by Eq. (18). We can therefore conclude that one cannot identify quasi-equilibrium just by observing the apparent recombination order in a transient experiment.

Note that under steady excitation, however, thermalization will always terminate since the quasi-Fermi-level is bounded from below due to the equilibrium density of excited carriers. The situation described in this section is thus not relevant for the description of steady excitation.

Table I compiles the results from Secs. III and III D by listing the apparent long-time recombination order for the shown DOS distributions and the two different pathways. Note that the asymptotic order depends on temperature for the exponential and the mixed DOS, while it is universally bimolecular for the Gaussian DOS.

TABLE I. Long-time apparent recombination orders for the DOS distributions used in Section III. In the case of free-trapped recombination in the mixed DOS, the recombination order is given by the DOS of the free carrier type. If the carrier type with the Gaussian DOS is free, the recombination order is 2.

	Gaussian DOS	Exponential DOS	Mixed
Free-trapped	2	$1+\varepsilon_0/kT$	2 or $1+\varepsilon_0/kT$
Free-free	2	$2\varepsilon_0/kT$	$1+\varepsilon_0/kT$

An important result of Sec. III is that the asymptotic expressions derived therein do not depend explicitly on time, but only on carrier densities. That, as we will address in Sec. VI, leads to the fact that the recombination orders in the case of steady excitation equal the asymptotic values from the transient paradigm.

IV. RELAXATION TIME OF THE RECOMBINATION ORDER

In this section we will calculate the characteristic time $\tau_{\rm rel}$ of the system reaching its asymptotic recombination order. We will treat the free-trapped recombination pathway here only. The behavior in case of free-free recombination is not shown here. A major difference between the two is that the case of a mixed DOS has to be treated separately for free-free recombination, while for the free-trapped case, it is the same as for the pure DOS of the respective free carrier type (cf. Sec. III C).

For free-trapped recombination in the exponential DOS, Orenstein and Kastner [25] showed that if $b_{\rm r} \lesssim b_{\rm t}$, the characteristic time of quasi-equilibration is

$$\tau_{\rm s} \simeq \frac{1}{\nu_0}\left[\frac{N_{\rm t}}{N(0)}\right]^{\varepsilon_0/kT}. \tag{34}$$

This is also the time of relaxation of the recombination order in this specific case ($\tau_{\rm rel}=\tau_{\rm s}$). Figure 5 shows that our calculated relaxation times are well described by Eq. (34).

However, as we saw in Sec. III D, although there is no quasi-equilibration in the case of $b_{\rm r} > b_{\rm t}$ in the exponential DOS, there is still an asymptotic constant recombination order. The timescale of approaching this asymptotics is τ as defined by Eq. (32).

For the Gaussian DOS, the relaxation time of the recombination order is given by the time when ε^* crosses ε_∞.

If $b_{\rm r} < b_{\rm t}$, or at high excitation intensities, where initially the quasi-Fermi-level is shallower than ε_∞, it can happen that ε^* reaches $\varepsilon_{\rm F}$ before ε_∞ [regime (ii)]. This will delay the establishment of the long-time bimolecular recombination order, which is only present when ε^* has reached ε_∞. When plotting the relaxation time over $N(0)$, this delay shows up as an s-shaped bending towards longer times (Fig. 6). The value of $N(0)$ at which the bend occurs, does not depend on $b_{\rm r}/b_{\rm t}$, but only on σ/kT, as can be seen from Fig. 6. Thus, experimentally varying the excitation intensity at known temperatures, one can determine σ from the position of the bend.

Of course, if recombination is so fast that it always prevents ε^* from reaching $\varepsilon_{\rm F}$, the bend will vanish. However, this is probably not the typical case in organic materials and heterostructures.

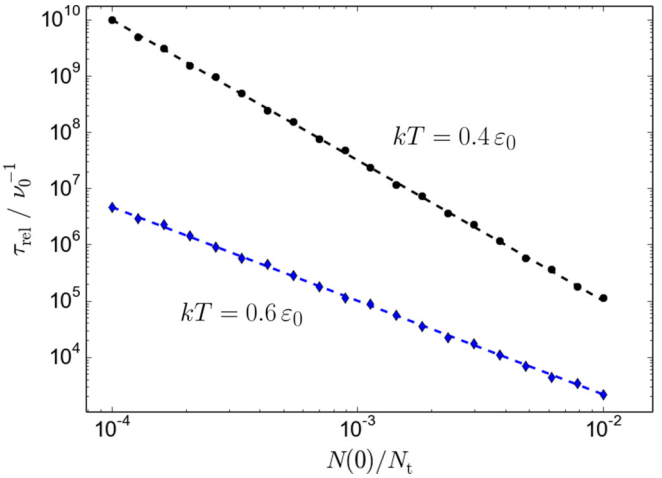

FIG. 5. Relaxation time $\tau_{\rm rel}$ of the recombination order as a function of the initial carrier density $N(0)$ in an exponential DOS for two different ε_0/kT. Symbols: Calculation from ε^* model. Here $\tau_{\rm rel}$ is defined as the crosspoint of the logarithmic part of $\varepsilon^*(t)$ with $\varepsilon_{\rm F}$ (see Fig. 9). In all calculations $b_{\rm r}/b_{\rm t} = 0.001$. The dashed lines are calculated from Eq. (34).

V. DENSITY OF CARRIERS RECOMBINING BEFORE RELAXATION

The fraction of carriers $f_{\rm rem}$ that remain in the sample at $t = \tau_{\rm rel}$ as calculated in Sec. IV is

$$f_{\rm rem} = N(\tau_{\rm rel})/N(0). \tag{35}$$

Also here we will restrict ourselves to the case of free-trapped recombination.

In the case of slow recombination in the exponential DOS, where a constant recombination order is established before

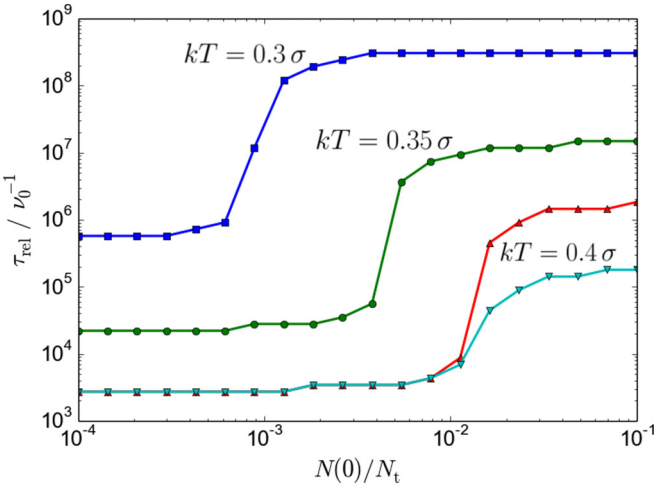

FIG. 6. Relaxation time $\tau_{\rm rel}$ of the recombination order as a function of the initial carrier density $N(0)$ in a Gaussian DOS for three different σ/kT. Here $\tau_{\rm rel}$ is defined as the first time that ε^* equals ε_∞. In all calculations $b_{\rm r}/b_{\rm t} = 0.001$, except for $kT = 0.4\,\sigma$, where also $b_{\rm r}/b_{\rm t} = 0.01$ is shown (▼).

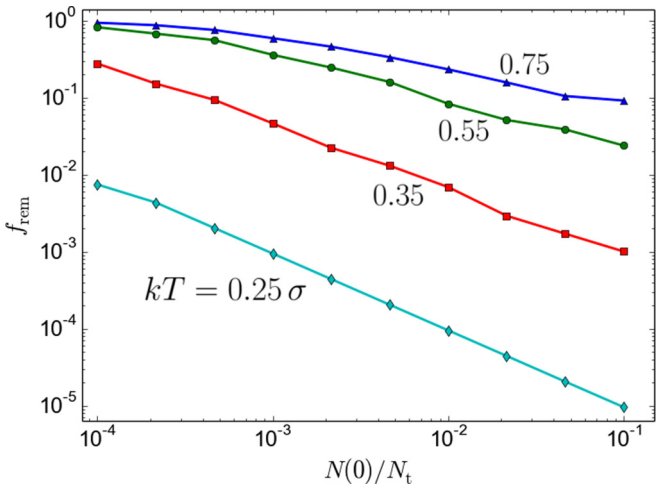

FIG. 7. Fraction $f_{\mathrm{rem}} = N(\tau_{\mathrm{rel}})/N(0)$ of carriers remaining at $t = \tau_{\mathrm{rel}}$ as a function of $N(0)/N_{\mathrm{t}}$ for four different σ/kT. For all calculations a Gaussian DOS and $b_{\mathrm{r}}/b_{\mathrm{t}} = 100$ was used.

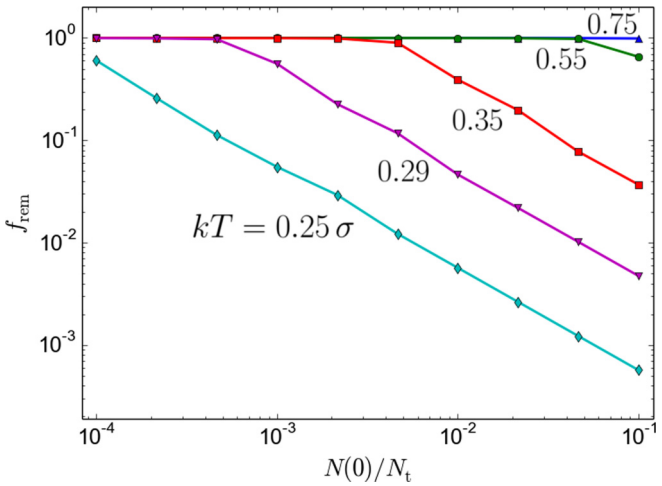

FIG. 8. Fraction f_{rem} of carriers remaining at $t = \tau_{\mathrm{rel}}$ as a function of $N(0)/N_{\mathrm{t}}$ for five different σ/kT. For all calculations a Gaussian DOS and $b_{\mathrm{r}}/b_{\mathrm{t}} = 0.01$ was used.

many charges had the chance to recombine, this fraction is always very close to unity.

Figure 7 shows f_{rem} as a function of initial excitation density for various reduced temperatures in a Gaussian DOS with fast recombination. Especially at low temperatures, the vast majority of carriers recombines before relaxation to the asymptotic recombination order is finished. With increasing temperature, f_{rem} increases and depends more weakly on $N(0)/N_{\mathrm{t}}$.

The reason for the increase is the fact that thermalization is faster at higher temperatures. Thus, less recombination can happen until τ_{rel}. The weakening of the dependence $\tau_{\mathrm{rel}}[N(0)/N_{\mathrm{t}}]$ with rising temperature can be rationalized as follows.

From Eqs. (6) and (9) we see that

$$\frac{dN}{dt} = -N^2 \exp[\varepsilon^*/kT]\frac{g(0)}{g(\varepsilon^*)}. \tag{36}$$

The dependence of dN/dt on N is of quadratic form, and strengthened or weakened exponentially by $1/kT$, which yields a weaker dependence at higher temperatures. The result is a weaker dependence of f_{rem} on $N(0)/N_{\mathrm{t}}$ for higher temperatures. The quadratic form of $n(N)$ only holds if ε^* does not depend on N. Before equilibration, this is only the case for $b_{\mathrm{r}} > b_{\mathrm{t}}$, where state filling is not influencing the thermalization dynamics.

Figure 8 depicts the opposite case. Here for low $N(0)/N_{\mathrm{t}}$, recombination only sets in after τ_{rel}. However, when $N(0)$ is increased, at some point ε_{F} rises above ε_∞ as described above and ε^* can reach ε_∞ only after enough charges have recombined so that $\varepsilon_{\mathrm{F}} = \varepsilon_\infty$ again. Thus, a kink appears, separating the constant f_{rem} at low $N(0)$ from f_{rem} decreasing like a power-law at high $N(0)$.

The position of the kink is given by

$$\varepsilon_{\mathrm{F}}(N) = \varepsilon_\infty = -\frac{\sigma^2}{kT}. \tag{37}$$

Thus, while the power-law does not depend on temperature, the position of the kink shifts to higher concentrations with increasing temperature, since ε_{F} has to rise higher at higher T to satisfy Eq. (37), which requires higher N.

This is a very useful notion since it allows to experimentally determine the point when ε_{F} equals ε_∞.

VI. STEADY-STATE RECOMBINATION AND IDEALITY FACTORS OF SOLAR CELLS

If the system is under steady excitation, the recombination (and, if applicable, extraction) current will at some point balance the generation current and a steady-state carrier density will be present. Thus, thermalization will eventually stop, when the deep states are filled by these steady-state carriers.

In the following, we will assume that the occupation function $f(\varepsilon)$ in this steady state is a Fermi-Dirac distribution.

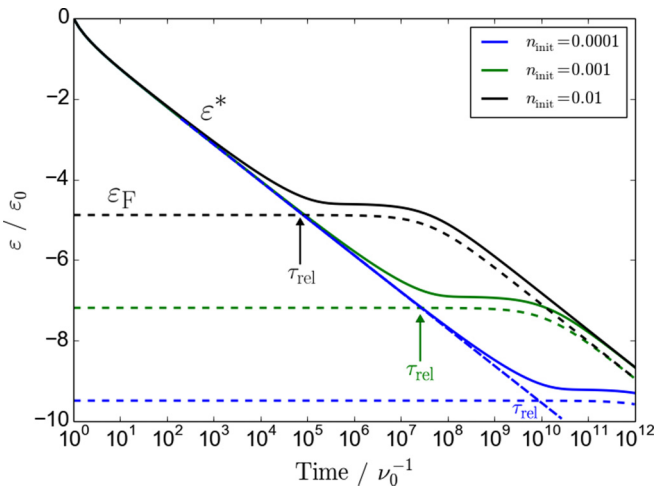

FIG. 9. Time development of ε^* compared to ε_{F} for three different initial carrier density fractions $n_{\mathrm{init}} = N(0)/N_{\mathrm{t}}$ in an exponential DOS with $kT = 0.4\,\varepsilon_0$ and $b_{\mathrm{r}} = 0.001\,b_{\mathrm{t}}$. The intersection of the logarithmic part (straight lines in this plot) of ε^* with ε_{F} defines the recombination order relaxation time τ_{rel} as plotted in Fig. 5.

In general, if recombination via trapped carriers plays a role, $f(\varepsilon)$ will differ from a Fermi-Dirac distribution. However, if only free carriers recombine with free carriers, we can show that this assumption is exact and quasi-equilibration will always occur:

If we consider constant generation of carriers and assume they are generated in random states, we have to add a generation term to Eq. (3). We will assume only free-free recombination and neglect the recombination term for trap states:

$$\frac{df(\varepsilon)}{dt} = [1 - f(\varepsilon)][b_t n(t) + G] - \nu_{\text{detrap}}(\varepsilon) f(\varepsilon), \tag{38}$$

with the constant generation rate G, measured in s^{-1}. If the system is in a steady state, the distribution of occupation probabilities $f(\varepsilon)$ will not change with time anymore. If we set $df/dt = 0$ in Eq. (38), we obtain

$$f(\varepsilon) = \frac{1}{1 + \frac{\nu_0}{b_t n + G} \exp\left[\frac{\varepsilon}{kT}\right]}, \tag{39}$$

which is a Fermi-Dirac distribution with the quasi-Fermi-level ε_F defined by

$$\exp\left[-\frac{\varepsilon_F}{kT}\right] := \frac{\nu_0}{b_t n + G}. \tag{40}$$

Since we are looking for the state where $f(\varepsilon)$ is constant, n has to be constant as well. Thus, a constant quasi-Fermi-level exists in the system

$$\varepsilon_F = -kT \ln \frac{\nu_0}{b_t n + G}. \tag{41}$$

For a solar cell under open-circuit conditions, the Shockley equation gives for the generation current J_{gen} [11,35,36]

$$J_{\text{gen}} = J_{\text{rec}} = J_0 \exp\left[\frac{eV_{\text{oc}}}{n_{\text{id}} kT}\right], \tag{42}$$

with the recombination current $J_{\text{rec}} = e\, d\, \frac{dN}{dt}$, the dark saturation current J_0, the elementary charge e, the open-circuit voltage V_{oc}, the device thickness d, and the so-called ideality factor n_{id}. n_{id} is introduced to describe deviations from the *ideal* Shockley diode equation, where $n_{\text{id}} = 1$.

Since the open-circuit voltage equals the difference of the hole and electron quasi-Fermi-levels, the electron and hole densities in the device depend exponentially on V_{oc}:

$$N = P = N_0 \exp\left[\frac{eV_{\text{oc}}}{2mkT}\right]. \tag{43}$$

Here the coefficient m depends on the DOS and the recombination mechanism.

In the following we will calculate m, δ, and n_{id} for the DOS combinations and recombination pathways discussed above.

A. Gaussian DOS

Let us assume that the quasi-Fermi-level in the steady state is situated well below ε_∞ for both electrons and holes. Then we can assume that almost all carriers have energies close to ε_∞. The carrier densities are then given by

$$N = N_0 \exp\left[-\frac{\varepsilon_{\infty,e} - \varepsilon_{F,e}}{kT}\right], \tag{44}$$

$$P = N_0 \exp\left[-\frac{\varepsilon_{F,h} - \varepsilon_{\infty,h}}{kT}\right]. \tag{45}$$

Combining Eqs. (44) and (45), we obtain

$$N = P = N_0 \exp\left[-\frac{E_{g,\text{eff}}}{2kT}\right] \exp\left[\frac{eV_{\text{oc}}}{2kT}\right], \tag{46}$$

where $E_{g,\text{eff}} = \varepsilon_{\infty,e} - \varepsilon_{\infty,h}$ is the effective energy gap. By comparing Eq. (46) to Eq. (43) we conclude that $m = 1$ for the purely Gaussian DOS. Remember that this result only holds if the $\varepsilon_{F,e/h}$ are closer to midgap than the $\varepsilon_{\infty,e/h}$.

While the value of m does not depend on if the recombining carriers are free or trapped, for the calculation of δ the interplay of free and trapped charge carriers has to be considered. However, in the Gaussian DOS for $\varepsilon_F < \varepsilon_\infty$ we know that $n \propto N$. In fact, Eqs. (13) and (14) still hold in quasi-equilibrium and $\delta = 2$ for the free-trapped and free-free recombination.

We finally calculate n_{id} by inserting Eqs. (13) and (14) into the recombination current from Eq. (42):

$$J_{\text{rec}} = e\, d\, \frac{dN}{dt} = -e\, d\, b_r N_0^2 \exp\left[-c\left(\frac{\sigma}{kT}\right)^2\right] \cdot \exp\left[-\frac{E_{g,\text{eff}}}{kT}\right] \exp\left[\frac{eV_{\text{oc}}}{kT}\right], \tag{47}$$

where $c = 1/2$ in the free-trapped and 1 in the free-free case. In both cases, comparison to Eq. (42) yields $n_{\text{id}} = 1$.

B. Exponential DOS

In the exponential DOS, almost all carriers are situated below ε_F and we can use Eq. (17) to express N and P

$$N = N_0 \exp\left[-\frac{\varepsilon_{t,e} - \varepsilon_{F,e}}{\varepsilon_0}\right], \tag{48}$$

$$P = N_0 \exp\left[-\frac{\varepsilon_{F,h} - \varepsilon_{t,h}}{\varepsilon_0}\right], \tag{49}$$

$$\Rightarrow N = P = N_0 \exp\left[-\frac{E_g}{2\varepsilon_0}\right] \exp\left[\frac{eV_{\text{oc}}}{2\varepsilon_0}\right]. \tag{50}$$

Here, $\varepsilon_{t,e/h}$ are the transport energies for electrons and holes, respectively. Comparison to Eq. (43) yields $m = \varepsilon_0/kT$ for the purely exponential DOS.

For determining δ, we can readily use Eqs. (19) and (22) since for their derivation we also assumed quasi-equilibrium. Moreover, we do not need to distinguish the different values of b_r/b_t since in the steady state, thermalization is always per definition stopped. We can thus conclude that in the exponential DOS, $\delta = 1 + \varepsilon_0/kT$ for the free-trapped and $2\varepsilon_0/kT$ for the free-free case.

The recombination current for the free-trapped case reads

$$J_{\text{rec}} = -e\, d\, b_r N_0^{1+\varepsilon_0/kT} N_t^{1-\varepsilon_0/kT} \cdot \exp\left[-\frac{E_g}{2}\left(\frac{1}{\varepsilon_0} + \frac{1}{kT}\right)\right] \exp\left[\frac{eV_{\text{oc}}}{2}\left(\frac{1}{\varepsilon_0} + \frac{1}{kT}\right)\right]. \tag{51}$$

An inspection of Eq. (51) and comparison to Eq. (42) yields

$$\frac{eV_{\rm oc}}{n_{\rm id}kT} \stackrel{!}{=} \frac{eV_{\rm oc}}{2}\left(\frac{1}{\varepsilon_0}+\frac{1}{kT}\right)$$
$$\Rightarrow \qquad n_{\rm id} = \frac{2}{1+kT/\varepsilon_0}. \tag{52}$$

Since typically $kT/\varepsilon_0 < 1$, $n_{\rm id}$ as given by Eq. (52) varies between 1 and 2. Analogous calculations for the free-free case result in $n_{\rm id} = 1$.

C. Mixed DOS

Finally, let us consider the combination of a Gaussian and an exponential DOS. For concreteness, we choose an exponential DOS for electrons and a Gaussian DOS for holes. In this case, we have to combine Eqs. (45) and (48) to yield

$$N = P = N_0 \exp\left[-\frac{E_{\rm g,eff}}{kT+\varepsilon_0}\right]\exp\left[\frac{eV_{\rm oc}}{2kT}\frac{2kT}{kT+\varepsilon_0}\right], \tag{53}$$

with $E_{\rm g,eff} = \varepsilon_{\rm t,e} - \varepsilon_{\infty,\rm h}$. Comparison to Eq. (43) yields $m = \frac{1}{2}(1+\frac{\varepsilon_0}{kT})$.

For the determination of δ we need to distinguish the possible recombination pathways. In the free-trapped case, we can just copy the values for free-trapped recombination in the purely exponential and Gaussian DOS: $\delta = 2$ for free holes and trapped electrons, $\delta = 1+\varepsilon_0/kT$ for free electrons and trapped holes. For free electrons and free holes recombining, we calculated the recombination order in quasi-equilibrium already in Sec. III C, where we again find $\delta = 1+\varepsilon_0/kT$.

The recombination currents for the different cases read as follows.

Free holes, trapped electrons:

$$J_{\rm rec} = -e\,d\,b_{\rm r}\,N_0^2 \exp\left[-\frac{1}{2}\left(\frac{\sigma}{kT}\right)^2\right]$$
$$\cdot \exp\left[-\frac{2E_{\rm g,eff}}{kT+\varepsilon_0}\right]\exp\left[\frac{eV_{\rm oc}}{kT}\frac{2kT}{kT+\varepsilon_0}\right]$$
$$\Rightarrow \qquad n_{\rm id} = m = \frac{1}{2}\left(1+\frac{\varepsilon_0}{kT}\right). \tag{54}$$

Trapped holes, free electrons:

$$J_{\rm rec} = -e\,d\,b_{\rm r}\,N_0^{1+\varepsilon_0/kT}\,N_{\rm t,e}^{1-\varepsilon_0/kT}$$
$$\cdot \exp\left[-\frac{E_{\rm g}}{kT}\right]\exp\left[\frac{eV_{\rm oc}}{kT}\right]$$
$$\Rightarrow \qquad n_{\rm id} = 1. \tag{55}$$

Free holes, free electrons:

$$J_{\rm rec} = -e\,d\,b_{\rm r}N_0^{1+\varepsilon_0/kT}\,N_{\rm t,e}^{1-\varepsilon_0/kT}\exp\left[-\frac{1}{2}\left(\frac{\sigma}{kT}\right)^2\right]\cdot$$
$$\cdot \exp\left[-\frac{E_{\rm g}}{kT}\right]\exp\left[\frac{eV_{\rm oc}}{kT}\right]$$
$$\Rightarrow \qquad n_{\rm id} = 1. \tag{56}$$

We summarize the results of Sec. VI in Table II. Note that for free-free recombination, $n_{\rm id}$ is always 1, independent of the DOS shape, while the recombination order δ can have values other than 2 and be even temperature dependent.

TABLE II. Steady-state parameters calculated in Sec. VI for the different DOS combinations. Here $\alpha = kT/\varepsilon_0$. f and t stand for *free* and *trapped*, respectively.

	m	δ	$n_{\rm id}$
Gaussian, f-t	1	2	1
Gaussian, f-f	1	2	1
Exponential, f-t	$1/\alpha$	$1+1/\alpha$	$2/(1+\alpha)$
Exponential, f-f	$1/\alpha$	$2/\alpha$	1
Mixed, $f_{\rm exp}$-$t_{\rm Gauss}$	$\frac{1}{2}(1+\frac{1}{\alpha})$	$1+1/\alpha$	1
Mixed, $t_{\rm exp}$-$f_{\rm Gauss}$	$\frac{1}{2}(1+\frac{1}{\alpha})$	2	$\frac{1}{2}(1+\frac{1}{\alpha})$
Mixed, f-f	$\frac{1}{2}(1+\frac{1}{\alpha})$	$1+1/\alpha$	1

When trapped charges in the exponential DOS play a role, even $n_{\rm id}$ is temperature dependent and greater than 1. Remarkably, for the Gaussian DOS the presence of ε_∞ always leads to bimolecular recombination with $n_{\rm id} = 1$. This relation, however, only holds if $\varepsilon_{\rm F}$ is lower than ε_∞, i.e., for not too high carrier densities.

VII. CONCLUSION

We show that recombination rates in materials with a broad DOS distribution measured after pulsed excitation are inherently time dependent since recombination gradually slows down as carriers relax in the DOS. When measuring the recombination order after pulsed excitation, this leads to an apparent high-order recombination at short times. As time goes on, the recombination order approaches an asymptotic value.

For the Gaussian and the exponential DOS distributions, this asymptotic value equals the recombination order of the equilibrated system under steady excitation, like a solar cell under operating conditions. For a more general DOS distribution, the transient and steady-state recombination order can also depend on the carrier density, depending on where the Fermi level is located in the DOS.

We want to stress that relaxation of the recombination order is not equivalent to thermal quasi-equilibration of the system itself. In some cases of the transient situations, like the case of $b_{\rm r} < b_{\rm t}$, these events coincide. In general, however, relaxation of the recombination order typically happens before equilibration of the whole system, if the latter happens at all.

Finally, interesting information about the DOS and the position of the Fermi level can be extracted from measuring the relaxation time of the recombination order and the fraction of carriers that have recombined until then as a function of temperature and excitation intensity.

ACKNOWLEDGMENTS

Financial support by the German Federal Ministry of Education and Research (Project No. UNVEiL) and the German Research Foundation (Project No. LE 747/48-1) is gratefully acknowledged. We also thank Dr. Steffen Roland (University Potsdam) and Prof. Karl Leo (TU Dresden) for fruitful discussions and support.

[1] H. Bässler, Phys. Status Solidi B **175**, 15 (1993).
[2] A. Devižis, A. Serbenta, K. Meerholz, D. Hertel, and V. Gulbinas, Phys. Rev. Lett. **103**, 027404 (2009).
[3] S. D. Baranovskii, Phys. Status Solidi B **251**, 487 (2014).
[4] A. Melianas, F. Etzold, T. J. Savenije, F. Laquai, O. Inganäs, and M. Kemerink, Nat. Commun. **6**, 8778 (2015).
[5] J. Orenstein and M. Kastner, Phys. Rev. Lett. **46**, 1421 (1981).
[6] M. Schubert, E. Preis, J. C. Blakesley, P. Pingel, U. Scherf, and D. Neher, Phys. Rev. B **87**, 024203 (2013).
[7] J. Lorrmann, M. Ruf, D. Vocke, V. Dyakonov, and C. Deibel, J. Appl. Phys. **115**, 183702 (2014).
[8] C. Tanase, E. J. Meijer, P. W. M. Blom, and D. M. de Leeuw, Phys. Rev. Lett. **91**, 216601 (2003).
[9] H. T. Nicolai, M. M. Mandoc, and P. W. M. Blom, Phys. Rev. B **83**, 195204 (2011).
[10] G. Garcia-Belmonte, P. P. Boix, J. Bisquert, M. Sessolo, and H. J. Bolink, Sol. Energy Mater. Sol. Cells **94**, 366 (2010).
[11] J. C. Blakesley and D. Neher, Phys. Rev. B **84**, 075210 (2011).
[12] T. Kirchartz and J. Nelson, Phys. Rev. B **86**, 165201 (2012).
[13] D. Rauh, C. Deibel, and V. Dyakonov, Adv. Funct. Mater. **22**, 3371 (2012).
[14] D. Hertel, H. Bässler, R. Guentner, and U. Scherf, J. Chem. Phys. **115**, 10007 (2001).
[15] V. R. Nikitenko, D. Hertel, and H. Bässler, Chem. Phys. Lett. **348**, 89 (2001).
[16] M. Westerling, C. Vijila, R. Österbacka, and H. Stubb, Phys. Rev. B **69**, 245201 (2004).
[17] J. Nelson, Phys. Rev. B **67**, 155209 (2003).
[18] J. Gorenflot, M. C. Heiber, A. Baumann, J. Lorrmann, M. Gunz, A. Kämpgen, V. Dyakonov, and C. Deibel, J. Appl. Phys. **115**, 144502 (2014).
[19] I. A. Howard, F. Etzold, F. Laquai, and M. Kemerink, Adv. Energy Mater. **4**, 1301743 (2014).
[20] J. Kurpiers and D. Neher, Sci. Rep. **6**, 26832 (2016).
[21] S. D. Baranovskii, P. Thomas, and G. J. Adriaenssens, J. Non-Cryst. Solids **190**, 283 (1995).
[22] G. J. Adriaenssens, S. D. Baranovskii, W. Fuhs, J. Jansen, and O. Öktü, Phys. Rev. B **51**, 9661 (1995).
[23] B. I. Shklovskii, H. Fritzsche, and S. D. Baranovskii, Phys. Rev. Lett. **62**, 2989 (1989).
[24] H. Cordes, G. H. Bauer, and R. Brüggemann, Phys. Rev. B **58**, 16160 (1998).
[25] J. Orenstein and M. Kastner, Solid State Commun. **40**, 85 (1981).
[26] A. Hofacker, J. O. Oelerich, A. V. Nenashev, F. Gebhard, and S. D. Baranovskii, J. Appl. Phys. **115**, 223713 (2014).
[27] M. Tachiya and K. Seki, Phys. Rev. B **82**, 085201 (2010).
[28] A. V. Nenashev, M. Wiemer, A. V. Dvurechenskii, L. V. Kulik, A. B. Pevtsov, F. Gebhard, M. Koch, and S. D. Baranovskii, Phys. Rev. B **95**, 104207 (2017).
[29] S. D. Baranovskii, T. Faber, F. Hensel, and P. Thomas, J. Phys. C **9**, 2699 (1997).
[30] D. Monroe, Phys. Rev. Lett. **54**, 146 (1985).
[31] V. I. Arkhipov, E. V. Emelianova, and G. J. Adriaenssens, Phys. Rev. B **64**, 125125 (2001).
[32] A. V. Nenashev, J. O. Oelerich, and S. D. Baranovskii, J. Phys.: Condens. Matter **27**, 093201 (2015).
[33] The excited system as a whole, containing generated holes and electrons, is per definition out of *strict* equilibrium.
[34] J. O. Oelerich, D. Huemmer, and S. D. Baranovskii, Phys. Rev. Lett. **108**, 226403 (2012).
[35] B. P. Rand, D. P. Burk, and S. R. Forrest, Phys. Rev. B **75**, 115327 (2007).
[36] W. J. Potscavage, A. Sharma, and B. Kippelen, Acc. Chem. Res. **42**, 1758 (2009).